

# High $P_T$ Higgs excess as a signal of non-local QFT at the LHC

Xing-Fu Su<sup>1</sup>, You-Ying Li<sup>1</sup>, Rosy Nicolaidou<sup>2</sup>, Min Chen<sup>1</sup>, Hsin-Yeh Wu<sup>1</sup>,  
Stathes Paganis<sup>a,1</sup>

<sup>1</sup> Department of Physics, National Taiwan University, No 1, Sec 4, Roosevelt Road, Taipei 10617, Taiwan

<sup>2</sup> IRFU, CEA, Universite Paris-Saclay, Gif-sur-Yvette; France

Received: date / Accepted: date

**Abstract** Non-local extensions of the Standard Model with a non-locality scale  $\Lambda_{NL}$  have the effect of smearing the pointlike vertices of the Standard Model. At energies significantly lower than  $\Lambda_{NL}$  vertices appear pointlike, while beyond this scale all beta functions vanish and all couplings approach a fixed point leading to scale invariance. Non-local SM extensions are ghost free, with the non-locality scale serving as an effective cutoff to radiative corrections of the Higgs mass. We argue that the data expected to be collected at the LHC phase 2 will have a sensitivity to non-local effects originating from a non-locality scale of a few TeV. Using an infinite derivative prescription, we study modifications to heavy vector-boson cross sections that can lead to an enhanced production of boosted Higgs bosons in a region of the kinematic phase space where the SM background is very small.

**Keywords** Computational methods and analysis tools, Hadron and lepton collider physics

**PACS** 29.85.FjData analysis · 14.80.BnStandard-model Higgs bosons

## 1 Introduction

Continuing searches at the Large Hadron Collider (LHC) have shown no evidence of new physics Beyond the Standard Model (BSM). The success of the SM suggests that the scale of new physics  $\Lambda_{NP}$  must be high enough when compared to the electroweak scale  $\Lambda_{EW}$ , so that its effect on the observed data be small. Modifications of SM cross sections at high momentum transfers (e.g. modifications of Higgs and  $W/Z$  boson yields), could

be the first sign of new physics and new heavy particles [1], [2].

A generic extension of the SM in which the particle interaction vertices are smeared is not a new idea [3]. A plethora of new physics scenaria involving new particles and new interactions can fit in such an effective description. To give a few examples: GUT theories [4–6], composite Higgs [7, 8], little Higgs [9–11], and models with vector  $Z'$  [12, 13], and  $W'$  [14]. Independent of the new physics behind this smearing, one can modify the pointlike behaviour by introducing higher derivatives in the kinetic terms of the SM Lagrangian or in the interaction vertices [15]. The simplest example is the smearing of a pointlike source represented by the Dirac delta function, by the exponential of an entire analytic function of derivatives:

$$e^{\alpha^2 \partial_x^2} \delta(x) = e^{\frac{\partial_x^2}{\Lambda^2}} \delta(x) = \frac{1}{\alpha \sqrt{2}} e^{-\frac{x^2}{4\alpha^2}}.$$

Application of this infinite sum of derivatives on the delta function, leads to the smearing of a pointlike to a Gaussian source. The energy scale at which smearing effects become important is  $\Lambda = 1/\alpha$ . Introduction of higher derivative terms in the Lagrangian leads to non-local effects that become relevant at a scale  $\Lambda \simeq \Lambda_{NL}$ . Extending the traditional QFT to a non-local version with a non-locality scale  $\Lambda_{NL}$  has several attractive features [15]. There are no new dynamical degrees of freedom other than the original ones of the corresponding local QFT, and the theory is UV finite. Beyond the non-locality scale all beta functions vanish, and all couplings approach a fixed point determined by  $\Lambda_{NL}$  [16, 17].

In practice, the non-local modification of the Lagrangian is achieved by introducing an infinite series of derivatives in the kinetic terms of the form:

$$e^{f(D^2)} = e^{\pm \frac{D^2}{\Lambda_{NL}^2}}, \quad (1)$$

<sup>a</sup>stathes.paganis@cern.ch, corresponding author

where  $D_\mu = \partial_\mu - igT^a A_\mu^a$  is the covariant derivative and  $D^2 = \eta_{\mu\nu} D^\mu D^\nu$ . This particular choice  $e^{f(D^2)}$  where  $f(D^2)$  is an entire analytic function, is required for avoiding the appearance of any extra poles in the propagator [15]. The fermionic part of the Lagrangian is modified as follows:

$$\mathcal{L} = i\bar{\psi} e^{\frac{D^2}{\Lambda_{NL}^2}} \gamma^\mu D_\mu \psi \quad (2)$$

In the limit  $\Lambda_{NL} \rightarrow \infty$  the original Lagrangian, in our case the SM, is recovered.

If we proceed to extend the SM Lagrangian to a non-local version (NL-SM) by introducing an infinite derivative sum in the kinetic terms, shown in Eq. 1, the result is a smearing of interaction vertices affecting relevant measured cross sections. The Drell-Yan  $ff \rightarrow \ell\ell$  process can set limits to the non-locality scale, in particular dilepton measurements at the LHC for dilepton invariant mass  $M_{\ell\ell} > 1$  TeV [18], [19], [20]. At the very high energies offered at the LHC, the weak gauge-boson scattering  $VV \rightarrow VV$  is dominated by the longitudinal degrees of freedom. So, effectively this scattering is Higgs-Higgs field scattering. In these processes the  $VVV$ ,  $VVH$  vertices may not be pointlike as a consequence of the new BSM physics. It should be stressed that non-locality in this context does not mean that the spacetime is discontinuous. Here we still consider a continuous spacetime, while non-locality is introduced through the presence of form factors due to new interactions appearing at a TeV or multi-TeV scale.

While approaching the non-locality scale from a lower energy, the interaction vertices appear smeared, and the theoretical treatment/modeling is typically done using form factors. This picture is similar to low energy electron-proton scattering where as the  $Q^2$  increases, the non-pointlike nature of the proton is revealed. Non-local modification approaches have also been used in nuclear reactions to explain proton-deuteron scattering data [21]. Theoretical models that can lead to such form factors have been proposed in the literature and many are gravity or string motivated [22], [23]. In string field theory  $a' = 1/\Lambda_{NL}^2$ , is the universal Regge slope. In the case of gravity, non-locality may appear at a Grand Unification scale at energies close to the Planck scale, while in the case of the SM, non-locality in the TeV scale is due to new particles and new interactions present at this scale. Thus one still needs to explain the origin of such non-locality, with compositeness being a good candidate.

New heavy vector bosons with masses close to the new physics scale  $\Lambda_{NL}$  appear in many BSM scenarios. In composite models they are expected to be present as the  $J = 1$  poles of a  $\rho$ -like Regge trajectory. In this

work, we propose to study the effects of non-local QFT modification on heavy vector-boson triplets (HVT). The impact of smeared vertices on these heavy states is to change their production cross section and their mass lineshape. In non-local QFT theories as in [3], [15], the modification enters through an exponential factor of the usual form:  $e^{\pm D^2/\Lambda_{NL}^2}$ , where the scale of new physics  $\Lambda_{NL}$  can be approximated by the pole mass of the heavy vector boson. Depending on the sign of the exponential and the mass of the heavy vector boson with respect to the non-locality scale, this factor has the effect to increase or decrease the cross-section predicted by the local theory and change the lineshape of the resonance. The actual effect depends on the details of the new physics and only measurements of these modifications can provide more information about the new theory.

In this paper, we first introduce the non-local QFT approach and summarize the potential impact of recent LHC results. In Section 3 we present an analysis used to search for heavy vector triplets at the LHC, and we report on the search potential for anomalous boosted Higgs production in association with weak gauge bosons as a function of the luminosity and the non-locality scale  $\Lambda_{NL}$ . Finally we conclude in Section 4.

## 2 Signals of Non-locality and Constraints from Data

Non-local modification of the SM leads to modifications of SM cross sections. The Drell-Yan dilepton cross section may receive positive corrections of the following general form [3]:

$$\sigma_{NL-SM} = e^{a(s/\Lambda_{NL}^2)} \times \sigma_{SM}, \quad (3)$$

where  $s$  is the square of the dilepton invariant mass, and  $a$  is a real factor that generalizes the  $\pm 1$  factor of Eq. 1. Using the full datasets from the Run 2 of LHC, one can already place upper limits to a hypothetical non-locality scale. Dilepton data from ATLAS and CMS extend out to an invariant mass of about 2.2 TeV [18], [19], [20]. In this work we assume positive  $a > 0$  and highlight the potential of the DY process in constraining the non-locality scale  $\Lambda_{NL}$ . It should be stressed that the actual extraction of limits or excesses using data is left to the LHC experiments. Using Eq. 3, predicted Drell-Yan modifications are presented in Fig. 1 for  $a = 1$  and varying values of the non-locality scale  $\Lambda_{NL}$ . In Fig. 1 the expected data  $1\text{-}\sigma$  combined uncertainty for an integrated luminosity of  $137 \text{ fb}^{-1}$  is shown, based on the yields in the same  $M_{\ell\ell}$  bins presented in [20]. For dilepton masses above 2 TeV the

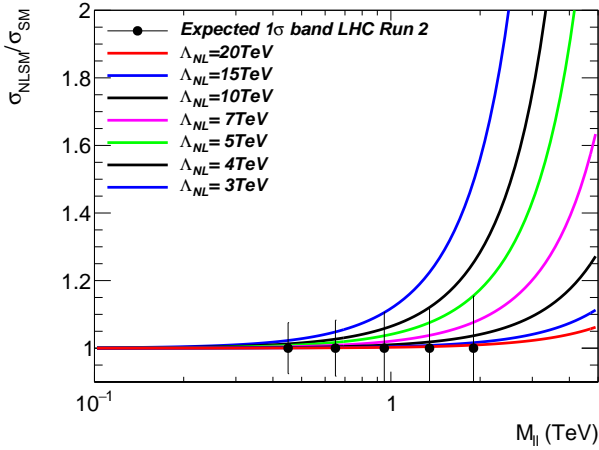


**Fig. 1** Drell-Yan dilepton cross-section modification with respect to the SM prediction due to non-local effects for an integrated luminosity of  $137 \text{ fb}^{-1}$ . The expected statistical and systematic uncertainties from a measurement at the LHC are also shown [20]. Based on these expectations, present and future measurements at the LHC can place constraints in the non-locality scale  $\Lambda_{\text{NL}}$ .

data statistical uncertainty becomes dominant. Examining Fig. 1, we see that a single LHC experiment can already place significant constraints on the non-locality scale  $\Lambda_{\text{NL}}$  at the level of a few TeV. The current level of deviation of the data from expectation is left to the experiments to determine.

As discussed in the introduction, non-locality can cause distortions to theoretically motivated broad heavy vector resonances. Broad resonances or a continuum of states are particularly interesting because their decays to dileptons are suppressed and the main decay mode is the diboson  $VH$  and  $VV$  [1]. In particular, the  $VH$  channel offers a unique signal of a very high  $P_T$  Higgs produced in association with a weak gauge boson, with very low SM background expectation. It is thus worthwhile to explore the potential of such a search and develop a method to produce heavy vector bosons with their lineshapes and cross sections modified by the non-locality scale. A straightforward approach is to use the HVT model, [24], that is also employed by the LHC experiments and then modify the predicted cross sections using Eq. 3. The HVT model is briefly summarized below.

HVT is a general phenomenological Lagrangian that can be used for the modeling of resonances predicted by a wide range of BSM scenarios. The Lagrangian describing the interactions of these resonances  $V^{a'}$ ,  $a = 1, 2, 3$  with quarks, leptons, vector bosons and the Higgs bo-

son is shown below:

$$\mathcal{L}_V^{\text{int}} = -\frac{g^2 c_F}{g_V} V_\mu^{a'} \bar{q}_k \gamma^\mu \frac{\sigma_a}{2} q_k - \frac{g^2 c_F}{g_V} V_\mu^{a'} \bar{\ell}_k \gamma^\mu \frac{\sigma_a}{2} \ell_k - g_V c_H \left( V_\mu^{a'} H^\dagger \frac{\sigma_a}{2} i D^\mu H + \text{hc} \right),$$

where  $q_k$  and  $\ell_k$  are the quark and lepton weak doublets,  $H$  is the Higgs doublet and  $\sigma^a$  the three Pauli matrices. In this Lagrangian, the HVT triplet  $V^{a'} = (W^{+'}, W^{-'}, Z')$  interacts with the Higgs doublet, i.e. the longitudinal degrees of freedom of the SM  $W$  and  $Z$  bosons and the SM Higgs, with a coupling strength  $g_V$ . In order to allow for a broader class of models, this coupling strength can be varied by the parameter  $c_H$ , so in the Lagrangian the full coupling to the SM weak and Higgs bosons is  $g_V c_H$ . The HVT resonances also couple to the SM fermions, again through their coupling to the SM weak and Higgs bosons,  $g^2/g_V$ , where  $g$  is the SM  $SU(2)_L$  weak gauge coupling. This coupling between HVT resonances and fermions is also controlled by an additional parameter  $c_F$  to allow for a broader range of models to be included, as follows:  $g^2 c_F/g_V$ . In this work, we use the so-called Drell-Yan scenario B, also used by the experiments [25]. This is a strongly coupled scenario as in composite Higgs models with  $\frac{g^2 c_F}{g_V} = 0.14$  and  $g_V c_H = -2.9$ , where the  $V'$  resonances are broader than in weakly coupled scenarios. For  $|g_V c_H| > 3$ , the resonance intrinsic width becomes significant and cannot be neglected. For such large couplings, the HVT resonance  $VH$  decay mode dominates while the di-fermion mode is heavily suppressed. The phenomenological implications of  $VH$  mode decay dominance have been discussed in [1].

In Fig. 2 sample  $Z'$  resonance DY cross sections as calculated from the HVT model and modified by the form factor of Eq. 3 are shown. The non-locality scale  $\Lambda_{\text{NL}}$  has been set at the pole mass  $M(Z')$ . Due to the presence of the factor  $e^{a(s/\Lambda_{\text{NL}}^2)}$ , the  $Z'$  lineshapes receive significant non-local modifications and are distorted. This is shown in Fig. 3 where the HVT model is used, and in Fig. 4 where the non-local modification is applied (NL-HVT). The potential increase of the cross section can lead to measureable anomalous Higgs boson production at very high  $P_T$ . One can notice the presence of long low mass tails coming from the parton density functions.

The HVT predicted lineshape and cross-section modification in the presence of a nearby non-locality scale  $\Lambda_{\text{NL}}$ , leads to a rich phenomenology. Depending on the number of resonances, their masses and widths, the impact on the  $VH$  and  $VV$  production at high momentum transfers could be significant. Thus, the interesting possibility that LHC phase-2 measurements could probe energy scales of order 10 TeV, is worth exploring.

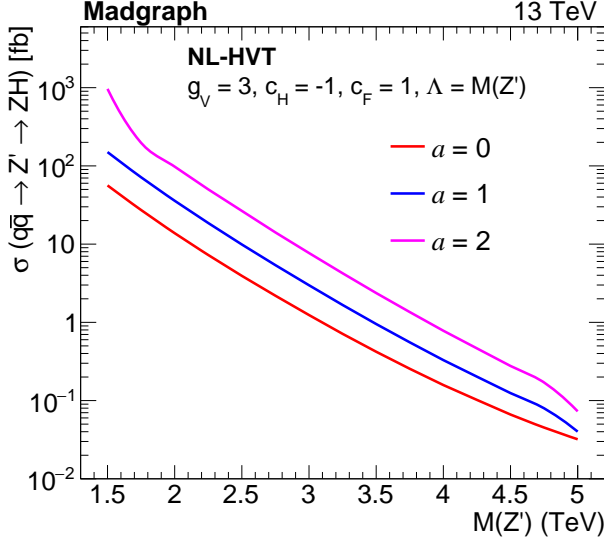


**Fig. 2**  $Z'$  resonance cross sections for the DY production mode after a non-local modification, as a function of the pole mass  $M(Z')$ . The non-locality scale  $\Lambda_{NL}$  in Eq.3 has been set at the pole mass  $M(Z')$ .

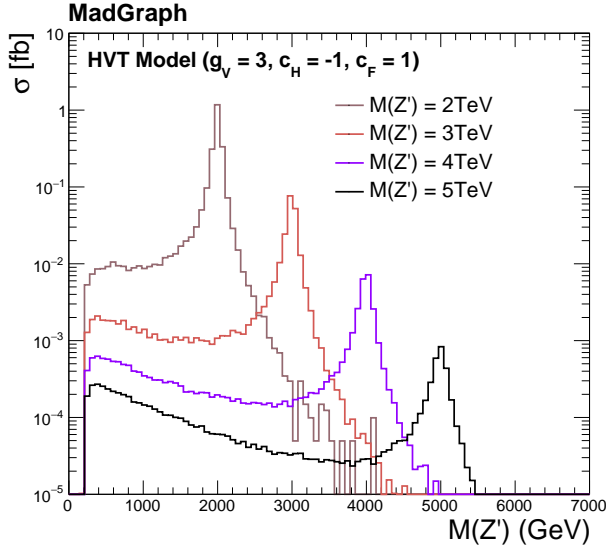


**Fig. 3** Leading order  $Z'$  resonance differential cross sections  $d\sigma/dM(Z')$  as predicted from the HVT model.

The diphoton system opening angle  $\Delta R$  and transverse momentum  $P_T$  are key variables sensitive to non-local effects. In Fig. 5 the Higgs yields as a function of the diphoton  $P_T$  are shown for  $Z'$  masses of 2, 3, 4 and 5 TeV. The SM Higgs prediction is shown in yellow and demonstrates that at high transverse  $P_T$ , its contribution becomes very small. The Higgs yields as a function of the diphoton  $\Delta R$  are shown in Figures 6 and 7 before any transverse momentum selection and after a  $P_T > 800$  GeV cut, respectively. Although the opening angle between the two photons originating from the

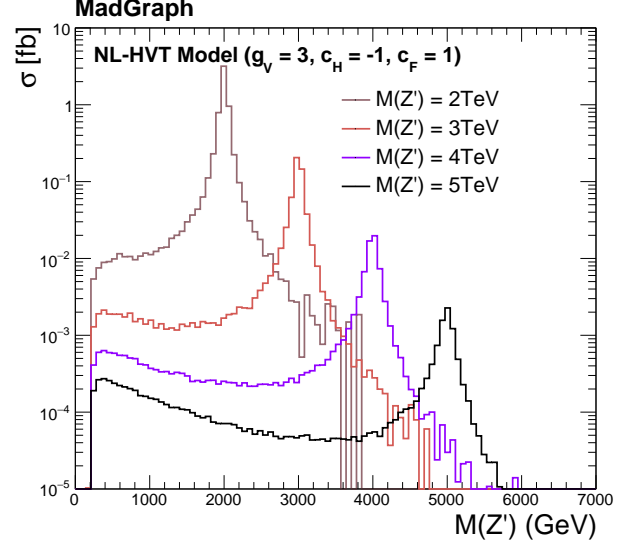


**Fig. 4** Leading order  $Z'$  resonance differential cross sections  $d\sigma/dM(Z')$  as predicted from the HVT model modified by the non-local form factor of Eq. 3 with  $a = 1$ .

Higgs decay is typically small, we can see that even for higher  $Z'$  masses, the photons are still separated by  $\Delta R > 0.15$ . Such levels of angular separation allow the reconstruction of two close-by high- $P_T$  photon clusters in the electromagnetic calorimeter. The presence of a pair of high- $P_T$  photons in the detector with an invariant mass close to 125 GeV, is a signal for new physics.

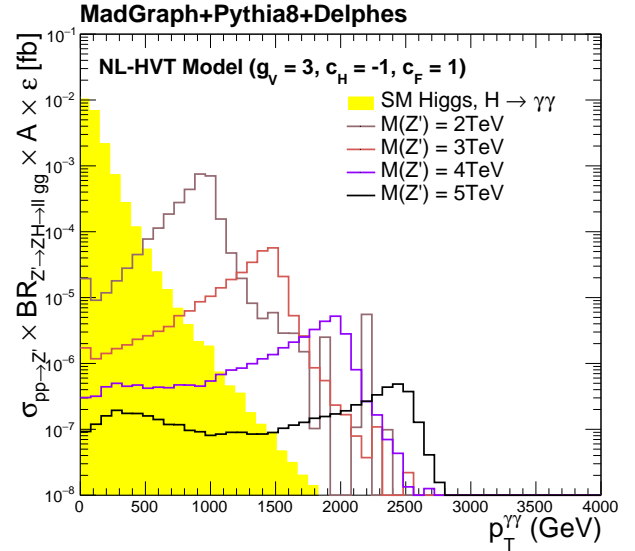


**Fig. 5**  $Z' \rightarrow ZH \rightarrow \ell\ell\gamma\gamma$  Higgs yields with respect to diphoton transverse momentum  $dN/dP_T^{\gamma\gamma}$ , in fb, as predicted from the non-local form factor in Eq. 3 with  $a = 1$ . The expected SM Higgs yield for the same selection is overlayed in yellow.

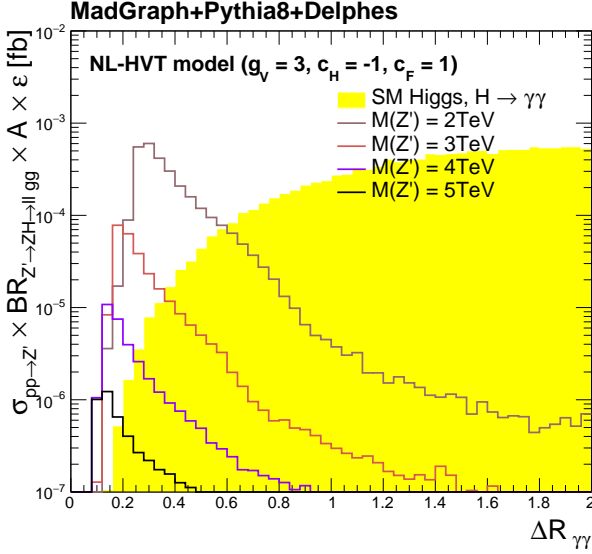


**Fig. 6**  $Z' \rightarrow ZH \rightarrow \ell\ell\gamma\gamma$  Higgs yields with respect to  $\Delta R_{\gamma\gamma}$ ,  $dN/d\Delta R_{\gamma\gamma}$ , in fb, as predicted from the non-local form factor in Eq. 3 with  $a = 1$ . The expected SM Higgs yield for the same selection is overlaid in yellow.

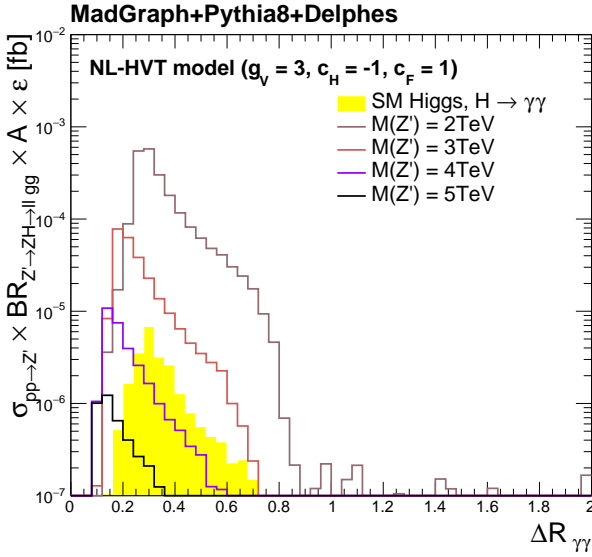


**Fig. 7**  $Z' \rightarrow ZH \rightarrow \ell\ell\gamma\gamma$  Higgs yields with respect to  $\Delta R_{\gamma\gamma}$ ,  $dN/d\Delta R_{\gamma\gamma}$ , in fb, after a diphoton transverse momentum cut of  $P_T > 800\text{ GeV}$ , as predicted from the non-local form factor in Eq. 3 with  $a = 1$ . The expected SM Higgs yield for the same selection is overlaid in yellow.

### 3 Sensitivity of a search at LHC

The observable that can serve as an early signal of non-locality at the LHC is the anomalous production of Higgs bosons at very high  $P_T$ . Although the  $H \rightarrow b\bar{b}$  is a potentially powerful decay channel for measuring such anomalous production, for Higgs  $P_T > 1\text{ TeV}$  the sensitivity drops due to the merging of the two  $b$  jets in a single jet. The efficiency of identifying small opening

angle  $b\bar{b}$  pairs falling into a single fat jet drops fast with the transverse  $P_T$ . In addition, for a single  $b\bar{b}$  jet, the QCD background is quite significant.

In the case of the diphoton channel, although the branching ratio  $H \rightarrow \gamma\gamma$  is 213 times lower than the  $H \rightarrow b\bar{b}$ , the photon pairs are potentially separable even at very high Higgs  $P_T$  while the diphoton identification efficiency is very high. The expected small continuum background from diphoton pairs at 125 GeV, the very small SM Higgs yields, and the excellent diphoton mass resolution lead to a competitive sensitivity when compared to  $H \rightarrow b\bar{b}$ . We argue that the observation of even a single high  $P_T$  diphoton pair with invariant mass close to the Higgs mass, would be statistically significant. Considering that the anomalous Higgs production could be produced by a broad heavy resonance or a continuum, one can proceed with the reconstruction of its full invariant mass distribution. However, this would require a large number of signal events. The search we propose has a SM Higgs background expectation that is at least one order of magnitude lower than the signal, aiming in observing at the LHC phase 2 the first signs of new physics by looking for events that have very small likelihood to be SM-induced. In this work we propose a search for boosted Higgs bosons decaying into two photons in association with a weak gauge boson.

To evaluate the expected signal yields for a broad range of masses and widths, we rely on Monte Carlo samples generated with MadGraph5, [26], interfaced to PYTHIA [27]. To simulate the response of an LHC-like experiment, realistic resolution and reconstruction efficiencies for electrons, muons, photons and jets were applied with the Delphes framework [28]. The specific cut-based event selection was based on a simplification of the cuts performed by LHC experiments on SM  $VH$  searches with  $H \rightarrow \gamma\gamma$  [29]:

- We require at least two photon candidates with the two leading candidates having  $P_T^{\gamma 1} > m_{\gamma\gamma}/3$  and  $P_T^{\gamma 2} > m_{\gamma\gamma}/4$ .
- The diphoton invariant mass must be in the range  $120 < m_{\gamma\gamma} < 130\text{ GeV}$ , called the signal region.
- Two opposite sign leptons with  $P_T^{\ell 1} > 30\text{ GeV}$  and  $P_T^{\ell 2} > 30\text{ GeV}$  are required for the  $ZH$  case, and a single lepton with  $P_T^{\ell 1} > 30\text{ GeV}$  for the  $WH$  case.
- For the  $ZH$  mode, the dilepton invariant mass is restricted to be close to the  $Z$  pole mass:  $80 < m_\ell < 110\text{ GeV}$ .

The difference between this selection and the SM diphoton reconstruction is that in our case the two photons have a small opening angle, so any photon isolation cuts have to be relaxed in order to preserve high reconstruction efficiency. An important additional requirement is a  $W'/Z'$  mass-dependent cut on the trans-

verse momentum of the  $\gamma\gamma$  system,  $P_T > M_{V'}/3$ , that selects highly boosted SM Higgs candidates. For such high diphoton  $P_T$ , both photons and leptons are also of very high transverse momentum and the event topology is really spectacular: two relatively small opening angle high  $P_T$  photons and two (one) high  $P_T$  leptons for the  $Z' \rightarrow ZH$  ( $W' \rightarrow WH$ ) channel. For such high  $P_T$  objects the single-object reconstruction efficiency is above 95% and most of the efficiency losses come from the event selection. The expected signal and background yields in units of fb are shown in Table 1. In the calculations shown in Table 1, the continuous background  $\ell\ell\gamma\gamma$  expectations are shown for a diphoton transverse momentum cut,  $P_T^{\gamma\gamma} > M_{V'}/3$ . A potentially significant background is the  $\ell\ell\gamma$  production with an additional fake photon, which is also included in the analysis. Fake rejection can only be estimated with full detector simulation and data, thus the  $\ell\ell\gamma$  prediction from the fast simulation is not realistic and results to an overestimation of this background. The final study and further cut optimizations are left to the LHC experiment groups.

Based on the results of Table 1, we conclude that for very high diphoton  $P_T$ , the SM Higgs production and the continuum background dominated by  $Z/W + \gamma\gamma$ , are the dominant backgrounds. Their contribution in the signal region of 120 – 130 GeV is rather small. The proposed analysis starts becoming sensitive for yields in the range of a few  $10^{-3}$  fb. This means that with an integrated luminosity of  $300 \text{ fb}^{-1}$  from the LHC phase 1, we should start observing very high  $P_T$  Higgs candidates recoiling off a dilepton or a single lepton. The High Luminosity LHC phase 2, is definitely in a better position to probe the NL-SM phase space, since we expect an integrated luminosity of  $3000 \text{ fb}^{-1}$ . However, signal yields are still in the sub-femtobarn level, thus requiring significant amounts of luminosity to observe a single event in the signal region.

The sensitivity of a search for non-local effects using high  $P_T$  Higgs as a probe, is presented as a function of the integrated luminosity and the scale of new physics in Figures 8 and 9 [30]. To fully scan the parameter space, we allow for the parameter  $a$  in Eq. 3 to vary. The case  $a = 0$  corresponds to the pure HVT model, i.e. absence of non-local modifications. From these results, one can see that the boosted Higgs  $VH$  leptonic mode can prove a powerful probe for anomalous high  $P_T$  Higgs production. For the high luminosities expected in the phase 2 of LHC the sensitivity of the search is expected to reach 4-5 TeV for  $a \simeq 1$ .

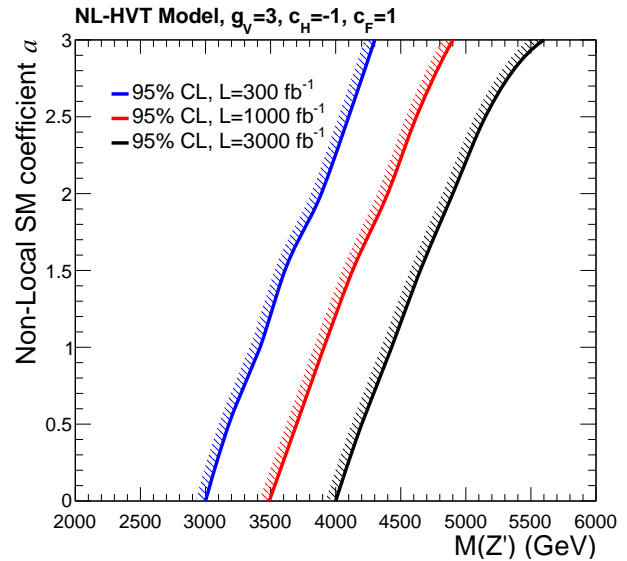


**Fig. 8** 95% Confidence Level limits in non-locality scale  $\Lambda_{NL}$  as a function of the parameter  $a$  and the integrated luminosity, based on measurements of anomalous Higgs production from a  $Z'$  resonance. Non-local modifications are obtained using the form factor  $e^{a(s/\Lambda_{NL}^2)}$ .

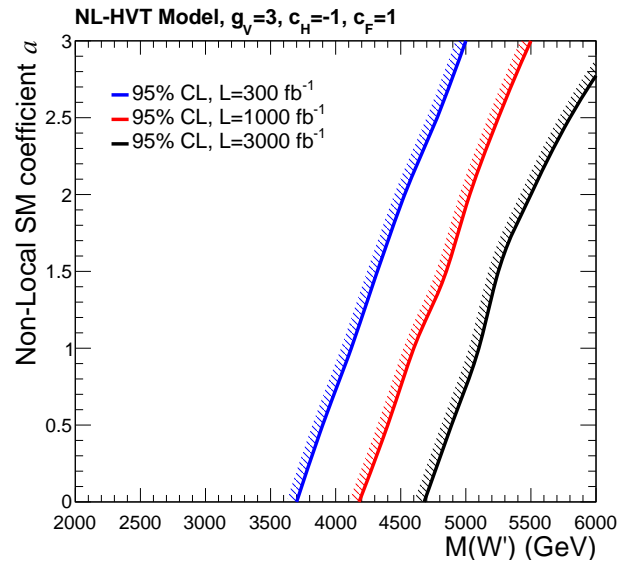


**Fig. 9** 95% Confidence Level limits in non-locality scale  $\Lambda_{NL}$  as a function of the parameter  $a$  and the integrated luminosity, based on measurements of anomalous Higgs production from a  $W'$  resonance. Non-local modifications are obtained using the form factor  $e^{a(s/\Lambda_{NL}^2)}$ .

## 4 Summary and Conclusions

In this work we explored the potential of observing early signs of non-local SM effects at the LHC. We have assumed that the non-locality scale is of order of a few TeV, and that at this scale heavy vector bosons are present. The heavy vector-boson cross section is modified by the presence of a non-local scale, leading to sig-

Process	$\sigma \times BR$ [fb]	$A \times \epsilon$ [%]	Yield ( $P_T^{\gamma\gamma} > M_{V'}/3$ ) [fb]	$M_{V'}$ [TeV]
$qq \rightarrow V' \rightarrow \gamma\gamma$				
$Z' \rightarrow ZH \rightarrow \ell\ell\gamma\gamma$ (2 TeV)	$1.90 \times 10^{-3}$	40.8	$6.8 \times 10^{-4}$	2
$Z' \rightarrow ZH \rightarrow \ell\ell\gamma\gamma$ (3 TeV)	$1.97 \times 10^{-4}$	34.4	$5.3 \times 10^{-5}$	3
$Z' \rightarrow ZH \rightarrow \ell\ell\gamma\gamma$ (4 TeV)	$2.99 \times 10^{-5}$	29.9	$5.1 \times 10^{-6}$	4
$Z' \rightarrow ZH \rightarrow \ell\ell\gamma\gamma$ (5 TeV)	$6.36 \times 10^{-6}$	29.4	$3.8 \times 10^{-7}$	5
$W' \rightarrow WH \rightarrow \ell\nu\gamma\gamma$ (2 TeV)	$1.26 \times 10^{-2}$	54.1	$6.0 \times 10^{-3}$	2
$W' \rightarrow WH \rightarrow \ell\nu\gamma\gamma$ (3 TeV)	$1.33 \times 10^{-3}$	46.7	$4.8 \times 10^{-4}$	3
$W' \rightarrow WH \rightarrow \ell\nu\gamma\gamma$ (4 TeV)	$1.99 \times 10^{-4}$	42.3	$4.8 \times 10^{-5}$	4
$W' \rightarrow WH \rightarrow \ell\nu\gamma\gamma$ (5 TeV)	$4.20 \times 10^{-5}$	43.8	$5.4 \times 10^{-6}$	5
SM $ZH \rightarrow \ell\ell\gamma\gamma$	0.20	13.3	$3.8 \times 10^{-5}$	2
SM $ZH \rightarrow \ell\ell\gamma\gamma$	0.20	13.3	$3.4 \times 10^{-6}$	3
SM $ZH \rightarrow \ell\ell\gamma\gamma$	0.20	13.3	$5.1 \times 10^{-7}$	4
SM $ZH \rightarrow \ell\ell\gamma\gamma$	0.20	13.3	$7.0 \times 10^{-8}$	5
SM $WH \rightarrow \ell\nu\gamma\gamma$	1.01	35.2	$2.7 \times 10^{-4}$	2
SM $WH \rightarrow \ell\nu\gamma\gamma$	1.01	35.2	$2.5 \times 10^{-5}$	3
SM $WH \rightarrow \ell\nu\gamma\gamma$	1.01	35.2	$3.3 \times 10^{-6}$	4
SM $WH \rightarrow \ell\nu\gamma\gamma$	1.01	35.2	$3.7 \times 10^{-7}$	5
SM Continuum $\ell\ell\gamma\gamma$	638.2	0.21	$2.7 \times 10^{-4}$	2
SM Continuum $\ell\ell\gamma\gamma$	638.2	0.21	$1.6 \times 10^{-5}$	3
SM Continuum $\ell\ell\gamma\gamma$	638.2	0.21	$2.8 \times 10^{-6}$	4
SM Continuum $\ell\ell\gamma\gamma$	638.2	0.21	$5.6 \times 10^{-8}$	5
SM Continuum $\ell\nu\gamma\gamma$	654.4	2.9	$5.2 \times 10^{-4}$	2
SM Continuum $\ell\nu\gamma\gamma$	654.4	2.9	$4.1 \times 10^{-5}$	3
SM Continuum $\ell\nu\gamma\gamma$	654.4	2.9	$3.4 \times 10^{-6}$	4
SM Continuum $\ell\nu\gamma\gamma$	654.4	2.9	$1.6 \times 10^{-7}$	5

**Table 1** Non-local anomalous Higgs production yields for  $a = 1$  in fb, compared to SM Higgs and continuum SM background yields for searches targeting resonance masses of 2, 3, 4 and 5 TeV.

nificant modification of their lineshape. Assuming the general case of resonances with finite width we calculate their cross sections using a simple model (HVT) that is modified by  $\sim e^{a(s/\Lambda_{NL}^2)}$  factors. Although the non-locality scale does not have to match the vector boson pole mass  $M_{V'}$ , observing that in the case of QCD the  $\rho$  mass is very close to the QCD transition scale, we have assumed  $M_{V'} = \Lambda_{NP}$ .

Possible modifications of dilepton invariant mass continuum at high  $Q^2$  already place constraints on non-local QFT, however the modifications of new heavy resonance lineshapes or their continuum could have more dramatic consequences due to their proximity to the new physics scale. The first signs of the presence of non-locality could be through the  $VH$  channel with the  $W/Z$  as well as the Higgs boson displaying TeV-level transverse momentum. This channel leads to very clean searches with small expected SM backgrounds. Although, in this work we focused on the single lepton and dilepton channels, the  $Z \rightarrow \nu\nu$  channel and the  $Z/W$  hadronic channels may significantly improve the search. In particular the  $Z \rightarrow \nu\nu$  channel can offer a spectacular signature of a boosted Higgs recoiling off a TeV-scale missing  $E_T$ .

Based on our results and due to the limitation of the LHC centre-of-mass energy, we only expect to probe

non-local effects if the relevant scale is not much higher than 5 TeV. At the LHC, a programme aimed at measuring Higgs production at very high  $P_T$  has already started, and the upcoming data from run 3 and LHC phase 2 are expected to probe locality at new record small distance scales.

## Acknowledgements

This work was supported by the Taiwanese Ministry of Science and Technology grant 109-2112-M-002-014-MY3.

## References

1. Y. Li, R. Nicolaïdou, S. Paganis, Exclusion of heavy, broad resonances from precise measurements of  $WZ$  and  $VH$  final states at the LHC, Eur. Phys. J. C 79(4), 348 (2019).
2. M. Hoffmann, A. Kaminska, R. Nicolaïdou, S. Paganis, Probing Compositeness with Higgs Boson Decays at the LHC, Eur. Phys. J. C 74(11), 3181 (2014).
3. T. Biswas and N. Okada, Towards LHC Physics with Non-local Standard Model, Nucl. Phys. B 898 (2015) 113-131.
4. J. C. Pati and A. Salam, Lepton Number as the Fourth Color, Phys. Rev. D 10 (1974) 275.
5. H. Georgi and S. Glashow, Unity of All Elementary Particle Forces, Phys. Rev. Lett. 32 (1974) 438.



6. H. Fritzsch and P. Minkowski, Unified Interactions of Leptons and Hadrons, *Annals Phys.* 93 (1975) 193.
7. E. Eichten and K. Lane, Low-Scale technicolor at the Tevatron and LHC, *Phys. Lett. B* 669 (2008) 235.
8. R. Contino, The Higgs as a Composite Nambu-Goldstone Boson, *arXiv:1005.4269 [hep-ph]* (2010).
9. T. Han, H. E. Logan, B. McElrath, and L.-T. Wang, Phenomenology of the little Higgs model, *Phys. Rev. D* 67 (2003) 095004.
10. M. Schmaltz and D. Tucker-Smith, Little Higgs Theories, *Ann. Rev. Nucl. Part. Sci.* 55 (2005) 229.
11. M. Perelstein, Little Higgs models and their phenomenology, *Prog. Part. Nucl. Phys.* 58 (2007) 247.
12. V. D. Barger, W.-Y. Keung, and E. Ma, A gauge model with light  $W$  and  $Z$  bosons, *Phys. Rev. D* 22 (1980) 727.
13. E. Salvioni, G. Villadoro, and F. Zwirner, Minimal  $Z'$  models: present bounds and early LHC reach, *JHEP* 09 (2009) 068.
14. C. Grojean, E. Salvioni, and R. Torre, A weakly constrained  $W'$  at the early LHC, *JHEP* 07 (2011) 002.
15. L. Buoninfante, G. Lambiase, A. Mazumdar, Ghost-free infinite derivative quantum field theory, *Nucl. Phys. B* 944 (2019) 114646.
16. A. Goshal, A. Mazumdar, and N. Okada, and D. Villalba, Non-local Non-Abelian Gauge Theory: Conformal Invariance and  $\beta$ -function, *arXiv:2010.15919 [hep-ph]* (2020).
17. A. Goshal, A. Mazumdar, and N. Okada, and D. Villalba, Stability of infinite derivative Abelian Higgs models, *Phys. Rev. D* 97, 7 (2017).
18. ATLAS Collaboration, Search for new non-resonant phenomena in high-mass dilepton final states with the ATLAS detector, *JHEP* 11 (2020) 005.
19. ATLAS Collaboration, Search for high-mass dilepton resonances using  $139\text{ fb}^{-1}$  of pp collision data collected at  $\sqrt{s} = 13\text{ TeV}$  with the ATLAS detector, *Phys. Lett. B* 796 (2019) 68.
20. CMS Collaboration, Search for resonant and nonresonant new phenomena in high-mass dilepton final states at  $\sqrt{s} = 13\text{ TeV}$ , *arXiv:2103.02708 [hep-ex]* (2021).
21. A. Ross, et. al., Effects of nonlocal potentials on (p,d) transfer reactions, *Phys. Rev. C* 92 (2015) 044607.
22. E. Witten, Noncommutative Geometry and String Field Theory, *Nucl. Phys. B* 268 (1986) 253.
23. D.A. Eliezer, R.P. Woodard, The Problem of Nonlocality in String Theory, *Nucl. Phys. B*, 325 389 (1989).
24. D. Pappadopulo, A. Thamm, R. Torre and A. Wulzer, Heavy Vector Triplets: Bridging Theory and Data, *JHEP* 09 (2014) 060.
25. ATLAS Collaboration, Combination of searches for heavy resonances decaying into bosonic and leptonic final states using  $36\text{ fb}^{-1}$  of proton proton collision data at  $\sqrt{s} = 13\text{ TeV}$  with the ATLAS detector, *Phys. Rev. D* 98 (2018) 5.
26. J. Alwall et. al. Madgraph 5 : Going beyond, *arXiv:1106.0522v1 [hep-ph]* (2011).
27. T. Sjostrand, S. Mrenna, P. Skands, A Brief Introduction to PYTHIA 8.1, *Comput. Phys. Commun.* 178 (2008) 852.
28. S. Ovin, X. Roubey, V. Lemaitre, DELPHES, a framework for fast simulation of a generic collider experiment, *arXiv:0903.2225 [hep-ph]* (2009).
29. CMS Collaboration, Measurements of Higgs boson production cross sections and couplings in the diphoton decay channel at  $\sqrt{s} = 13\text{ TeV}$ , *JHEP* 07, 027 (2021). *arXiv:2103.06956 [hep-ex]*.
30. G. Cowan, K. Cranmer, E. Gross, O. Vitells, Asymptotic formulae for likelihood-based tests of new physics, *Eur. Phys. J. C* 71, 1 – 19 (2011).